THE JOURNAL OF NAVIGATION (2017), **70**, 1153–1169.
doi:10.1017/S0373463317000261

A Main Peak Extraction Method for High-Order BOC Signals

Fang Liu and Yongxin Feng

(*School of Information Science and Engineering, Shenyang Ligong University, Shenyang, 110159, China*)
(E-mail: zhqing1019@163.com)

Binary Offset Carrier (BOC) modulation signals have been applied in Global Navigation Satellite Systems (GNSS) because they offer a higher positioning accuracy and higher multipath rejection. However, there is a drawback in that the autocorrelation functions have multiple side peaks, meaning that this technique also leads to the large main peak estimation error problem and a low correlation decision efficiency problem. In this paper, we propose a new Main Peak Extraction (MPE) method for high-order BOC signals to solve these problems. In the new method, the synthesis cross-correlation function is established, and the geometry graph is formatted to calculate the estimation main peak. We eliminate all side peaks and improve the main peak phase estimation precision under the condition that the sub-carrier phase is offset. The results of the simulation demonstrate that the new method can achieve better main peak decision efficiency, side peak cancellation ability and phase estimation performance than traditional methods.

KEYWORDS

1. GNSS. 2. Satellite Navigation. 3. BeiDou. 4. Software Receiver.

Submitted: 1 February 2016. Accepted: 10 April 2017. First published online: 30 May 2017.

1. INTRODUCTION. The rapid development of Global Navigation Satellite Systems (GNSS (Liu et al., 2015), e.g., BeiDou (Compass) (Liu, Pang et al., 2015; Sun et al., 2014), Galileo, GLONASS and the Global Positioning System (GPS)) brings great opportunities and challenges for signal synchronisation and receivers. Specifically, new modulation technologies have been applied in GNSS, e.g., the Binary Offset Carrier (BOC) modulation. BOC modulation technology has attracted much interest for new GNSS since it can provide a higher positioning accuracy and higher multipath rejection than the conventional Phase Shift Keying (PSK) modulation as well as a spectral separation from the existing GNSS. In BOC modulation, the signal is generated by multiplying a Pseudo Random Noise (PRN) code with a sub-carrier. With the emergence and application of the BOC modulation signal, high efficiency synchronous receiving technology has become the touchstone of research.

In general, the GNSS signal synchronous receiving system primarily includes acquisition and tracking processing. Fast course synchronisation for the frequency and phase

is performed in acquisition processing, and the acquisition parameters are then transited. Further precise synchronisation is performed by using the transition parameters in tracking processing. Although the tracking phase precision must be high and the acquisition phase precision is not high, with the high demand for GNSS reception, high precision acquisition is also increasingly receiving more attention. Furthermore, since the repetition rate of the tracking processing in the receiver is high, especially with the receiver in hot start mode, the result is that, if there are higher precision acquisition parameters, the overall efficiency of the tracking system will be greatly improved. Therefore, research on high precision acquisition technology is especially important.

Although acquisition accuracy and the signal autocorrelation function are closely related, only the centre main peak corresponds to the relevant function. The main problem with BOC signals is that their autocorrelation has multiple side-peaks around the main peak, which causes the large error problem of main peak estimation. Furthermore, the more the number of the side peaks increases with the modulation order, the smaller the spacing between the main and side peaks becomes, which causes the low efficiency problem of the main peak decision. Thus, main peak extraction technology has become especially important for high-order BOC signals, for example BOC (14,2) and BOC (15,2·5). Among them, the BOC (14,2) signal has been applied in the Chinese BeiDou B1 band, and the BOC (15,2·5) signal has been applied in the Chinese BeiDou B3 band.

Several techniques that have been reported to avoid these problems include the Bump-Jump (BJ) method (Fine and Wilson, 1999), Double Estimator (DE) method (Ward et al., 2003), and double phase estimator (DPE) method (Hodgart and Simons, 2012). The BJ method is not effective for high-order BOC signals or multipath conditions. Although the DE and DPE methods are useful for high-order BOC signals, high sampling frequency and tremendously high computational complexity restrict the low cost and miniaturization design of the receiver. To date, these preferable techniques can be grouped into the following categories: the BPSK-like technique (Martin et al., 2003; Betz, 2001; Burian et al., 2006), the Autocorrelation Side-Peak Cancellation Technique (ASPeCT) (Julien et al., 2007), Sub-Carrier Phase Cancellation (SCPC) (Heiries et al., 2005) Technique, and Side Peak Cancellation Technique (SPCT) (Yao and Feng, 2010; Yao et al., 2010; Sanghun et al., 2009).

While the BOC signal was treated as the sum of two BPSK signals, the BPSK-like method was proposed to provide an unambiguous correlation; several improved methods such as the Cyclically Shift and Combine (CSC) methods (Mao et al., 2013) have subsequently been proposed. This type of method can reduce sub-carrier influence, but the energy and necessary information are lost, and the sharpness of the main-peak is destroyed, severely degrading receiving performance.

The ASPeCT method can overcome the ambiguous characteristic, but it achieves only partial ambiguity mitigation (i.e., reduced but not completely attenuated side-peaks) at the cost of reduced discriminator pulling range. Furthermore, ASPeCT is only useful for BOC (n, n) cases.

Although the Sub-Carrier Cancellation (SCC) and Sub-Carrier Phase Cancellation (SCPC) technologies can ignore the effects of phase, they do not take advantage of the high-accuracy characteristics of the BOC signal. Moreover, the main peak estimation error is large, and the correlation decision efficiency is low; thus, they cannot provide high acquisition for tracking transition parameters.

The essence of SPCT is to minimise the side-peaks of the auto-correlation function since they are the origins of false lock tracking. The methods presented in Feng et al. (2014; 2015) have some drawbacks in the tracking stage because the effect of the side-peak is not removed completely. Thus, it can potentially lock onto the false original peak. A high precision process method (Brahim et al., 2015) is provided by combining different correlation functions, and a time-multiplexed double strobe scheme (Liu et al., 2015) for a Time Multiplexed Binary Offset Carrier (TMBOC) modulated signal is presented to improve synchronisation performance. However, the adaptabilities of these methods are deficient because they are not suited for high-order BOC signals.

2. MAIN PEAK EXTRACTION METHOD.

To tackle the abovementioned problems, we propose a new main peak extraction (MPE) method for high-order BOC signals. The essence of the MPE method is as follows: Local shifting sequences are defined according to the relationship between the sub-carrier and PRN code, and the synthesis cross-correlation function is then established to solve the sub-carrier influence in the MPE method. Furthermore, a reference frame is established using the minimum and maximum peaks of the synthesis cross-correlation function, and the geometry graph is formatted to calculate the estimation main peak. We now describe in detail the principle of the new method.

Firstly, the received digital intermediate frequency signal is modelled after the frequency down-conversion, power amplifying, Analog to Digital Converter (ADC), and band-pass filtering. It is approximately given as

$$R(n) = d(n)C(n)S_{CS}(n) = d(n)C(n)\mathrm{sgn}(\sin(2\pi\omega n + \theta)) \tag{1}$$

where $d(n)$ is the binary navigation data, $C(n)$ is the PRN code, $S_{CS}(n)$ is the sub-carrier sequence, which can also be expressed as $\mathrm{sgn}(\sin(2\pi\omega n + \theta))$, ω is the sub-carrier frequency, and θ is the sub-carrier phase offset. The BOC signal is usually expressed as BOC (f_1, f_2). We then define the sampling frequencies of the BOC signal, the frequency of the sub-carrier and the PRN code as f_S, f_{SC}, and f_C, respectively. The frequencies are expressed as

$$f_{SC} = f_1 \times 1{\cdot}023 \times 10^6 \tag{2}$$

$$f_C = f_2 \times 1{\cdot}023 \times 10^6 \tag{3}$$

Then ε is the number of half sub-carriers in one code chip, and is defined as the modulation order, which is expressed as Equation (4).

$$\varepsilon = \frac{2f_1}{f_2} \tag{4}$$

λ is the sampling number for the half sub-carrier and T is the sampling number in one code chip. These sampling numbers are expressed as Equations (5) and (6), respectively.

$$\lambda = \frac{f_S}{2f_{SC}} \tag{5}$$

$$T = \frac{f_S}{f_C} \tag{6}$$

https://doi.org/10.1017/S0373463317000261 Published online by Cambridge University Press

From Equation (1), we find that the main and side peaks will be distorted in the BOC autocorrelation function when θ is not equal to zero, that is, sub-carrier phase offset occurs in the received signal.

Thus, the local shifting sequences in the new method are defined to overcome the influence, which is given by

$$L_L(n) = C(n)S_C(n)E_L(n) = C(n)\text{sgn}(\sin(2\pi\omega n))E_L(n) \tag{7}$$

$$L_R(n) = C(n)S_C(n)E_R(n) = C(n)\text{sgn}(\sin(2\pi\omega n))E_R(n) \tag{8}$$

where $E_L(n)$ and $E_R(n)$ are expressed as Equations (9) and (10), respectively, in which k is a positive integer from one to infinity.

$$E_L(n) = \begin{cases} 1, & (k-1)\varepsilon\lambda \le n \le (k-1)\varepsilon\lambda + \lambda \\ 0, & (k-1)\varepsilon\lambda + \lambda < n < k\varepsilon\lambda \end{cases} \tag{9}$$

$$E_R(n) = \begin{cases} 0, & (k-1)\varepsilon\lambda < n < k\varepsilon\lambda - \lambda \\ 1, & k\varepsilon\lambda - \lambda \le n \le k\varepsilon\lambda \end{cases} \tag{10}$$

The signal received before processing is executed by circumferential correlation arithmetic function with $L_L(n)$ and $L_R(n)$, which are expressed as

$$X_L(n) = R(n) \otimes L_L(n) = d(n)C(n)\text{sgn}(\sin(2\pi\omega n + \theta)) \otimes C(n)\text{sgn}(\sin(2\pi\omega n))E_L(n) \tag{11}$$

$$X_R(n) = R(n) \otimes L_R(n) = d(n)C(n)\text{sgn}(\sin(2\pi\omega n + \theta)) \otimes C(n)\text{sgn}(\sin(2\pi\omega n))E_R(n) \tag{12}$$

where $\otimes$ is defined as the circumferential correlation arithmetic notation.

Thus, the synthesis cross-correlation function is established as

$$\Delta X(n) = \frac{f_{SC}}{f_C}(|X_L(n)| + |X_R(n)| - |X_L(n) - X_R(n)|) \approx \frac{f_{SC}}{f_C}\left(\wedge_0(n) + \sum_{i=T/2}^{T/2} \wedge_i(n)\right) \tag{13}$$

where $\wedge_0(n)$ and $\wedge_i(n)$ are trigonometric peaks, whose centres are at zero and i, respectively.

From Equation (13), it is possible to obtain the correlation result $\Delta X(n)$ which has many peaks. We find that the unadulterated main peak is influenced by some distortion peaks $\sum_{i=T/2}^{T/2} \wedge_i(n)$ in the correlation result. As there are many peaks in $\Delta X(n)$, we calculate the minimum peak in $\Delta X(n)$, which is defined as D.

$$D = \min[\Delta X(n)] \tag{14}$$

Where min[] is the minimum peak calculation function, the peak value of D is defined as D_x, and the peak position of D is defined as D_y.

Then the left maximum peak of D is defined as B, whose peak value is defined as B_x, and peak position is defined as B_y. The right maximum peak of D is defined as A, whose peak value is defined as A_x, and peak position is defined as A_y. Thus, we utilise D, B, and A to establish a reference frame, in which D_x, B_x, and A_x are used as the abscissa, D_y, B_y, and A_y are used as the ordinate. The reference frame is shown in Figure 1.

https://doi.org/10.1017/S0373463317000261 Published online by Cambridge University Press

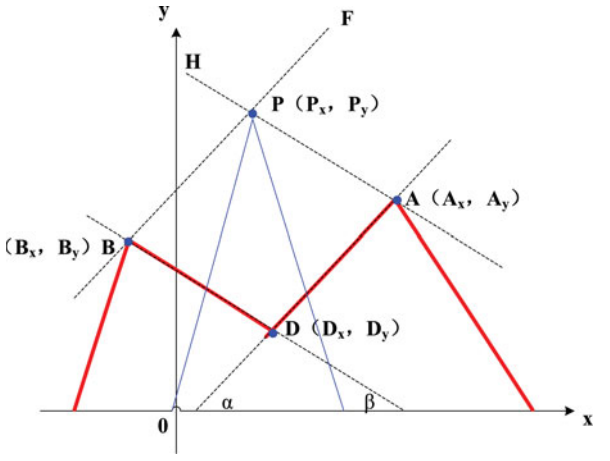

Figure 1. The theory of the structure reference frame.

In Figure 1, the angle between line and coordinate X is α, the angle between line BD and coordinate X is β, and the tangent functions of α and β are expressed as

$$K_\alpha = \frac{A_y - D_y}{A_x - D_x} \tag{15}$$

$$K_\beta = \frac{B_y - D_y}{B_x - D_x} \tag{16}$$

Thus, line BF is established as parallel to line AD. In the same way, line AH is established as parallel to line BD in Figure 1.

$$P_y - B_y = K_\alpha(P_x - B_x) \tag{17}$$

$$P_y - A_y = K_\beta(P_x - A_x) \tag{18}$$

Thus, when Equations (17) and (18) are combined, the crossing point P of lines BF and AH is formed, which is the estimation main peak of the MPE method. Then we subtract Equation (18) from Equation (17) to obtain Equation (19), which is the estimation main peak position P_x. From the multiplication result of Equation (17) and K_β, we subtract the multiplication result of Equation (18) and K_α to obtain Equation (20), which is the estimation main peak value P_y.

$$P_x = \frac{A_y - B_y + K_\alpha B_x - K_\beta A_x}{K_\alpha - K_\beta} \tag{19}$$

$$P_y = \frac{K_\beta K_\alpha A_x - K_\beta K_\alpha B_x + K_\beta B_y + K_\beta A_y}{K_\alpha - K_\beta} \tag{20}$$

3. SIMULATION AND ANALYSIS. The MPE method, the SCPC and SPCT methods are simulated and analysed using the following parameters. The high-order BOC signals

https://doi.org/10.1017/S0373463317000261 Published online by Cambridge University Press

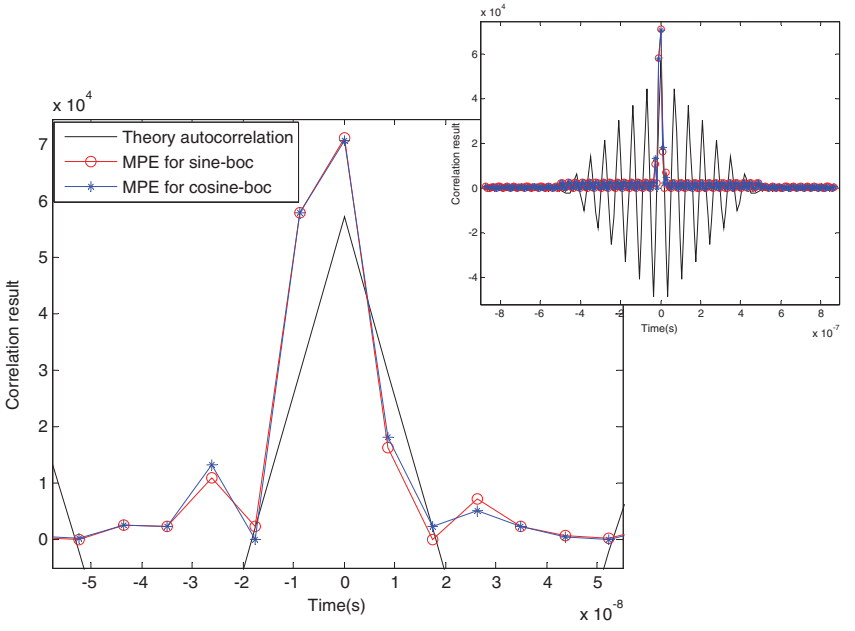

Figure 2. BOC (14,2) correlation results.

are selected as BOC (14,2) and BOC (15,2·5). The sampling frequencies, the frequency of the sub-carrier f_{SC} and the PRN code f_C are expressed as:

$$f_S = 120 \times 10^6 \tag{21}$$

$$f_{SC} = \begin{cases} 14 \times 1{\cdot}023 \times 10^6, & when\ BOC\ (14,2) \\ 15 \times 1{\cdot}023 \times 10^6, & when\ BOC\ (15,2{\cdot}5) \end{cases} \tag{22}$$

$$f_C = \begin{cases} 2 \times 1{\cdot}023 \times 10^6, & when\ BOC\ (14,2) \\ 2{\cdot}5 \times 1{\cdot}023 \times 10^6, & when\ BOC\ (15,2{\cdot}5) \end{cases} \tag{23}$$

3.1. *Main peak extraction analysis.* To verify the validity of the MPE method, the main peak extraction ability is analysed. The correlation results and their magnified picture for sine-BOC (14,2) and cosine-BOC (14,2) are shown in Figure 2, and the results for sine-BOC (15,2·5) and cosine-BOC (15,2·5) are shown in Figure 3. The results of the theoretical autocorrelation have multiple side peaks, but the correlation of the MPE method has only one main peak. From the magnified figures, we find that the main peak position of the MPE method is the same as the theory position, and the correlation results for sine-BOC and cosine-BOC are approximately the same. The results demonstrate that the side peaks can be cancelled in the MPE method and that the main peak can be extracted in the correct position.

3.2. *Performance comparison analysis.* Firstly, we define the maximum peak to average ratio to verify the synchronisation and receiver ability, and the main peak decision efficiency, which, being the ratio of the maximum and average peaks, is expressed as P_m/P_a. Main peak decision efficiency increases with P_m/P_a. We then define the main-side

https://doi.org/10.1017/S0373463317000261 Published online by Cambridge University Press

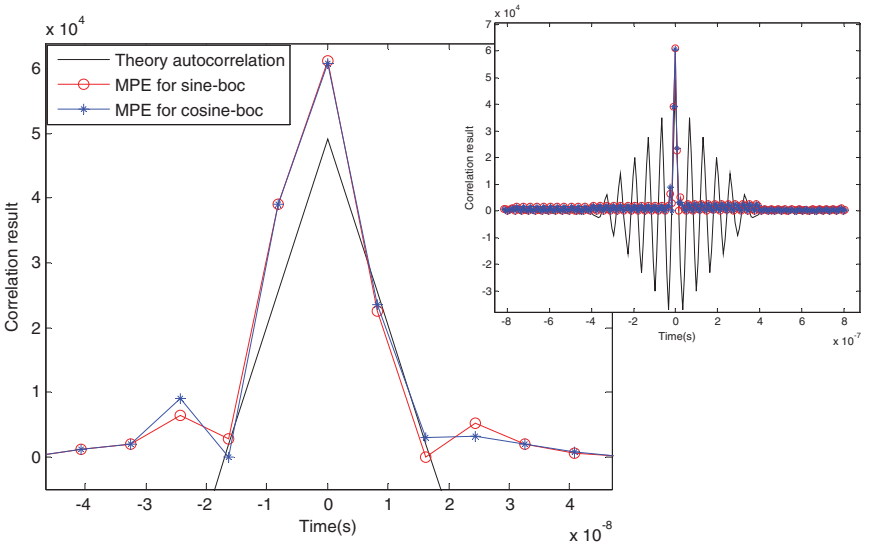

Figure 3. BOC (15,2·5) correlation results.

peak ratio to test the ability of the side peak inhibition, which, being the ratio of the main and side peaks, is expressed as P_m/P_s; side peak inhibition ability increases with P_m/P_s. Furthermore, since the main peak estimation error is a very important indicator, we will test and express it as P_e. Synchronisation ability increases as P_e decreases. Based on the definition of P_m/P_a, P_m/P_s and P_e, the MPE method is compared with other preferable methods, namely, the SCPC and SPCT methods.

As the effect of phase is smaller, the sub-carrier phase offset can be ignored in certain methods but is inevitable in the receiving signal. Thus, with changing sub-carrier phase offset, P_m/P_a results for BOC (14,2) and BOC (15,2·5) are shown in Figure 4. The results show that the peak to average ratio of the MPE method is the greatest, demonstrating that the MPE method's main peak decision efficiency and synchronisation ability are the best. With changing sub-carrier phase offset, P_m/P_s results are shown in Figure 5, whose results show that the main-side peak ratio of the MPE method is noticeably greater than that of the other two methods. Thus, the side peak inhibition ability of the MPE method is demonstrably the best. Furthermore, with changing sub-carrier phase offset, P_e results are shown in Figure 6, in which the average phase estimation error of the MPE method is the smallest, which demonstrates that this method's phase estimation performance is the best.

We know the difference between sine-BOC and cosine-BOC is different sub-carrier phase. From Figures 4, 5 and 6, we find that the sub-carrier phase offset has no obvious effect on P_m/P_a, P_m/P_s, and P_e. Thus, we take sine-BOC as an example to analyse the related results in the following simulations.

Furthermore, under the various noise conditions, P_m/P_a, P_m/P_s and P_e are also simulated to verify the environment adaptability. With changing Signal to Noise Ratio (SNR), P_m/P_a results are shown in Figure 7, and P_m/P_s results are shown in Figure 8. The results show that the peak to average ratio of three methods increases with SNR, and the MPE method is higher than the other two methods under the same condition. From Figure 8, it can also be observed that the main-side peak ratio of the MPE method noticeably increases

https://doi.org/10.1017/S0373463317000261 Published online by Cambridge University Press

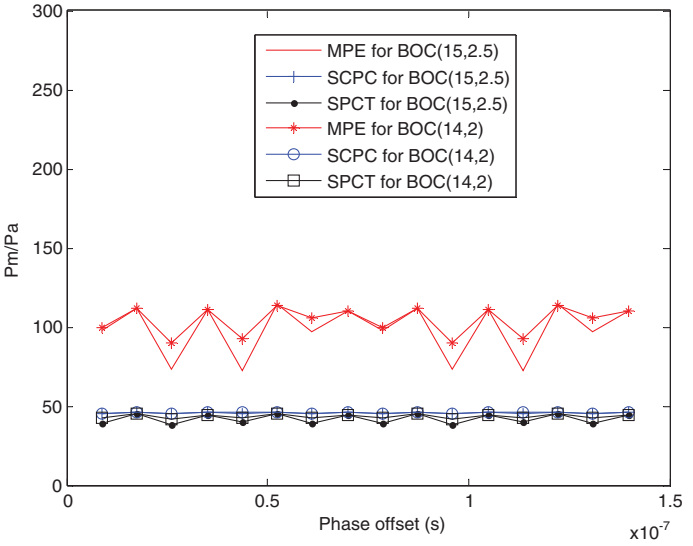

Figure 4. P_m/P_a results with changing sub-carrier phase offset.

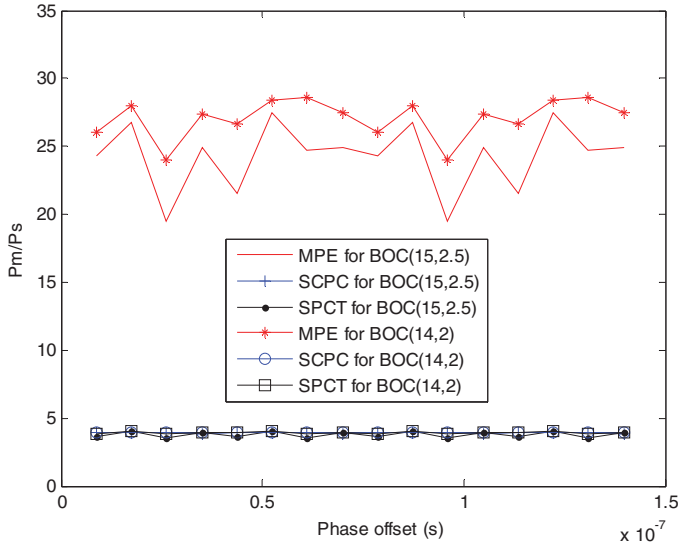

Figure 5. P_m/P_s results with changing sub-carrier phase offset.

with SNR, that change is not noticeable with an SNR increase in the case of the SCPC and SPCT methods, and that the results are higher with the MPE method than with the other two methods. Thus, the MPE method's main peak decision efficiency is the best, and the side peak cancellation ability is also the best under the same SNR condition.

P_e results with changing SNR are then shown in Figure 9, whose results show that the phase estimation error of the MPE method is noticeably better than that of the other two methods and that the estimation error of the SCPC and SPCT methods is larger when

https://doi.org/10.1017/S0373463317000261 Published online by Cambridge University Press

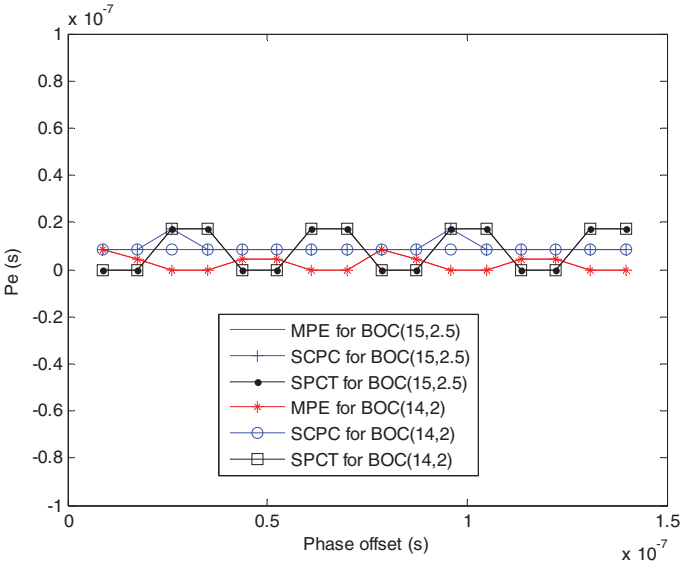

Figure 6. P_e results with changing sub-carrier phase offset.

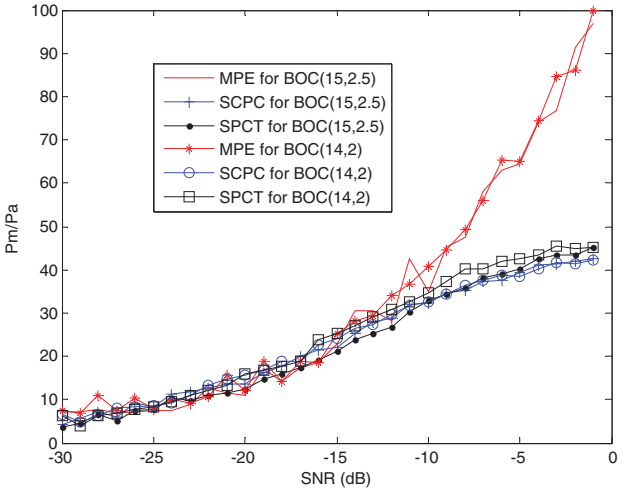

Figure 7. P_m/P_a results with changing SNR.

SNR is less than −25 dB, which demonstrates that the MPE method's phase estimation performance is the best under the same condition.

Since the frequency error is inevitable in RF filtering processing and mix-frequency processing, the comparison tests of the three methods are also analysed when there is a frequency error in the receiving signal. P_m/P_a results with changing frequency error are shown in Figure 10, and P_m/P_s results are shown in Figure 11. From Figure 10, it can be observed that the peak to average ratio for the three methods decreases as the frequency error increases. When P_m/P_a is 10, the frequency error adaptive range is 1 KHz for the

https://doi.org/10.1017/S0373463317000261 Published online by Cambridge University Press

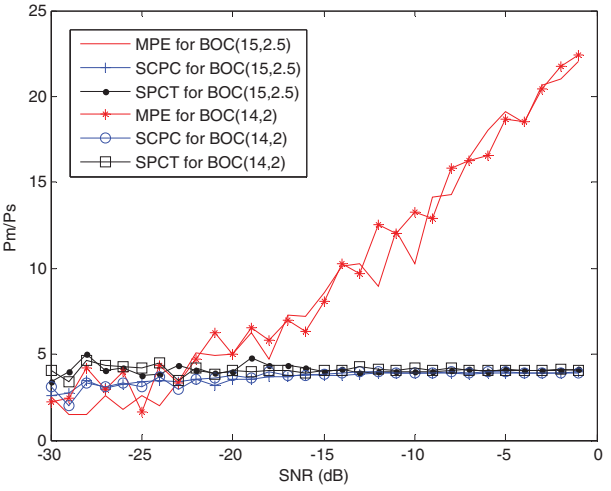

Figure 8. P_m/P_s results with changing SNR.

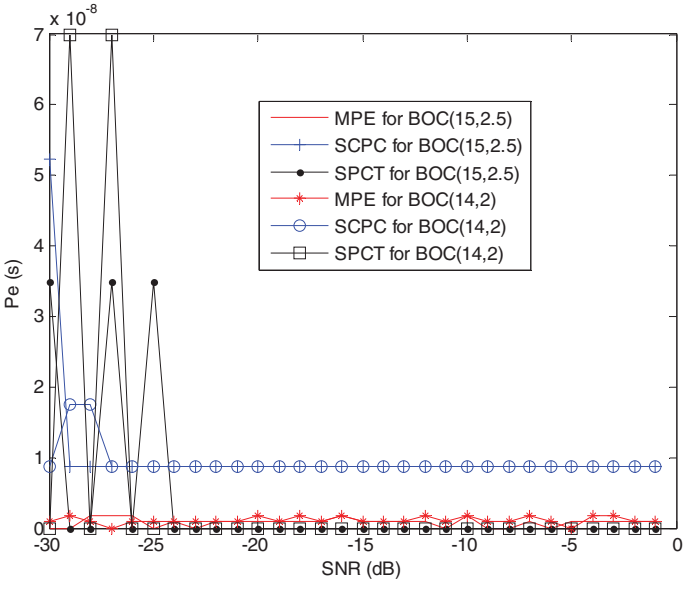

Figure 9. P_e results with changing SNR.

SCPC method, 1·5 KHz for the SPCT method, and 2 KHz for the MPE method, respectively. Moreover, the MPE method is noticeably better than the other two methods under the same frequency error condition. From Figure 11, it can be observed that the main-side peak ratio of the MPE method noticeably decreases as the frequency error increases, that changes are not noticeable as the frequency error increases in the case of the SCPC and SPCT methods and that the MPE method is noticeably better than the other two methods under the same frequency error condition. Thus, the side peak cancellation ability of the MPE method is noticeably better than that of the other two methods.

https://doi.org/10.1017/S0373463317000261 Published online by Cambridge University Press

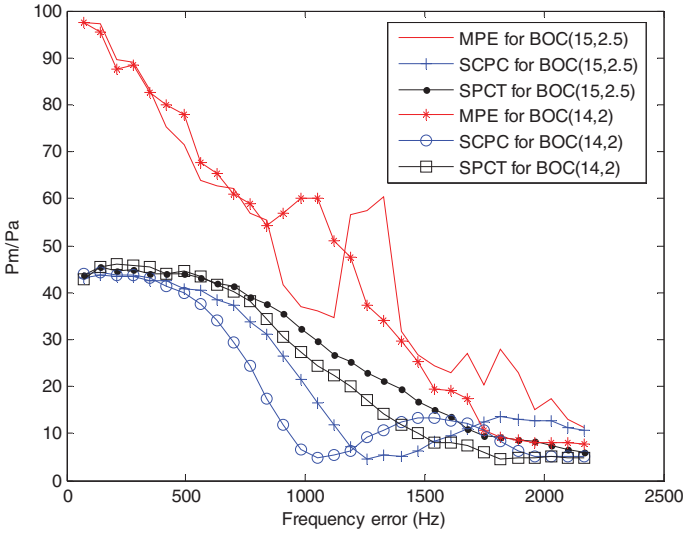

Figure 10. P_m/P_a results with changing frequency error.

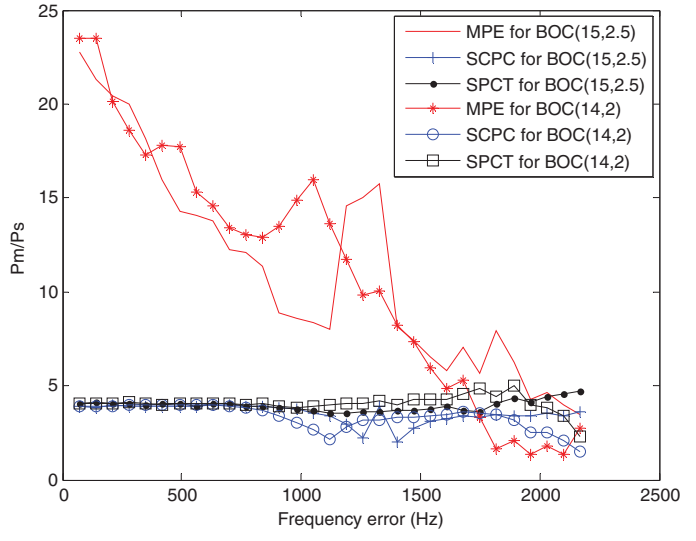

Figure 11. P_m/P_s results with changing frequency error.

In addition, P_e results with changing frequency error are shown in Figure 12, whose results show that the phase estimation error of the SCPC and SPCT methods becomes greater when the frequency error is 1 KHz, 1·8 KHz, respectively. However, the phase estimation error of the MPE method is very small when the frequency error is less than 2 KHz. Thus, these results demonstrate that the frequency error adaptive ability of the new method is the best.

In light of the real complex environmental characteristics, especially with respect to different interference signals and multipath errors, these methods are also tested under

https://doi.org/10.1017/S0373463317000261 Published online by Cambridge University Press

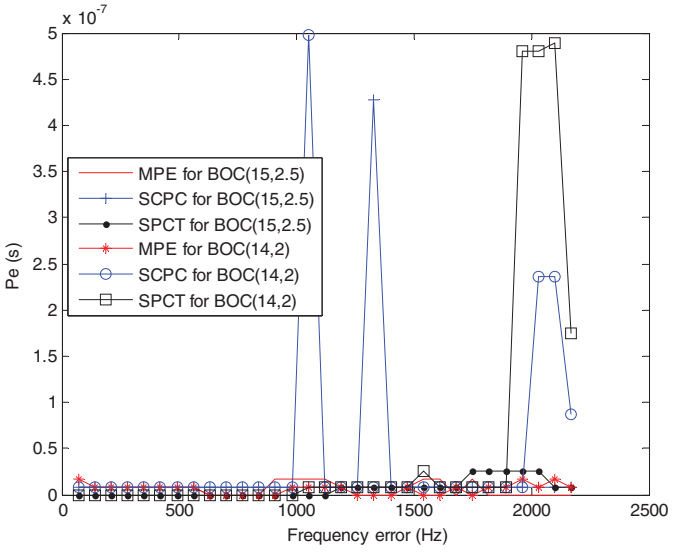

Figure 12. P_e results with changing frequency error.

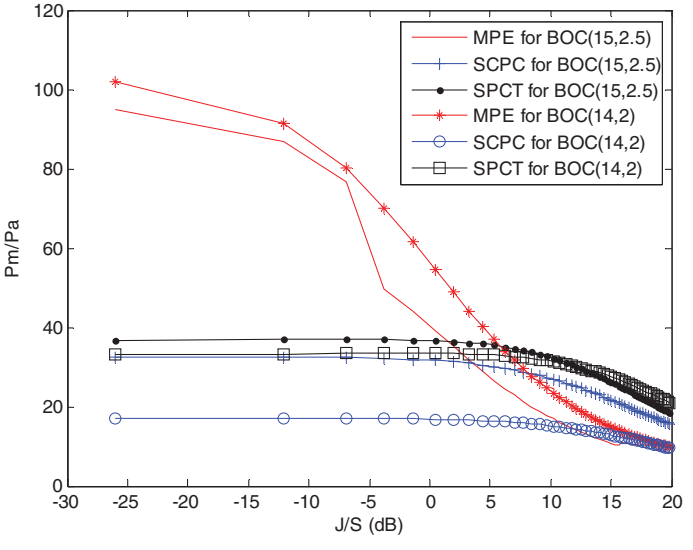

Figure 13. P_m/P_a results with changing J/S.

the mixed complex signals condition. We defined J/S, which is the power ratio of the mixed complex signals and receiving signal. P_m/P_a results with changing J/S are shown in Figure 13, and P_m/P_s results are shown in Figure 14. From Figure 13, it can be observed that the peak to average ratio of the three methods decreases as J/S increases and that the MPE method is better than the other two methods under the same J/S condition. From Figure 14, it can be observed that the main-side peak ratio of the MPE method noticeably decreases as J/S increases, that changes are not noticeable as J/S increases in the case of

https://doi.org/10.1017/S0373463317000261 Published online by Cambridge University Press

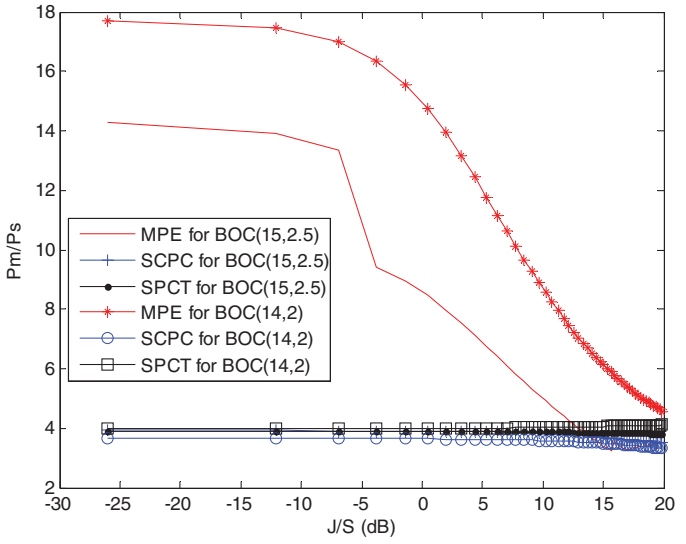

Figure 14. P_m/P_s results with changing J/S.

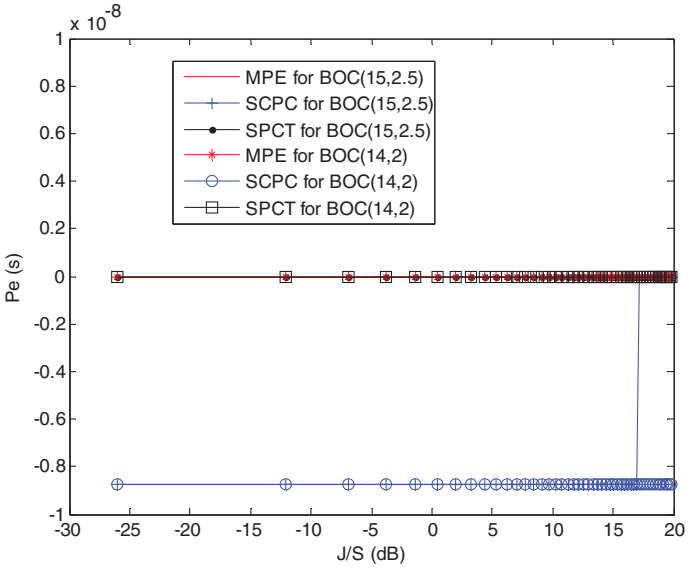

Figure 15. P_e results with changing J/S.

the other two methods, and that the MPE method is noticeably better than the other two methods. Moreover P_e results with changing J/S are shown in Figure 15, whose results show that the phase estimation error of the three methods is very small; however, the phase estimation error of the SCPC method is the largest.

In addition, P_m/P_a results with changing different phases of indirect signal are shown in Figure 16, P_m/P_s results are shown in Figure 17, and P_e results are shown in Figure 18. It can be observed that the peak to average ratio of the MPE method is better than the other

https://doi.org/10.1017/S0373463317000261 Published online by Cambridge University Press

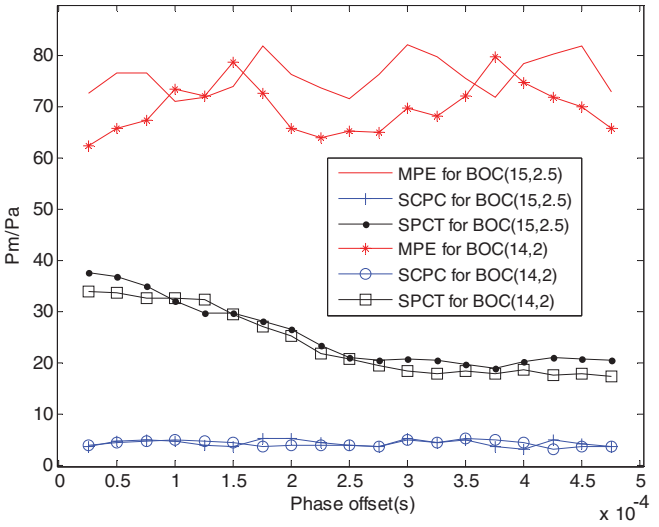

Figure 16. P_m/P_a results with changing phases of indirect signal.

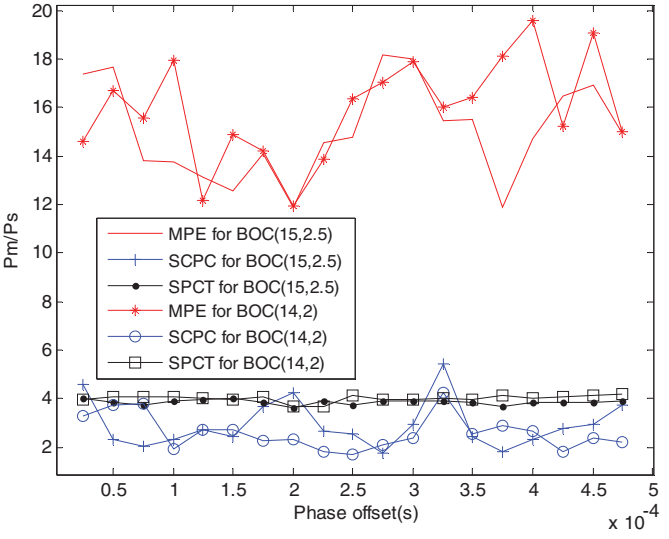

Figure 17. P_m/P_s results with changing phases of indirect signal.

two methods, and that the main-side peak ratio of the MPE method is noticeably better than the other two methods under the same condition. The results also show that the phase estimation error of the three methods is very small; however, the phase estimation error of the SCPC method is the largest. These results demonstrate that the MPE method's main peak decision efficiency, side peak cancellation ability and phase estimation performance are all the best under the same conditions.

https://doi.org/10.1017/S0373463317000261 Published online by Cambridge University Press

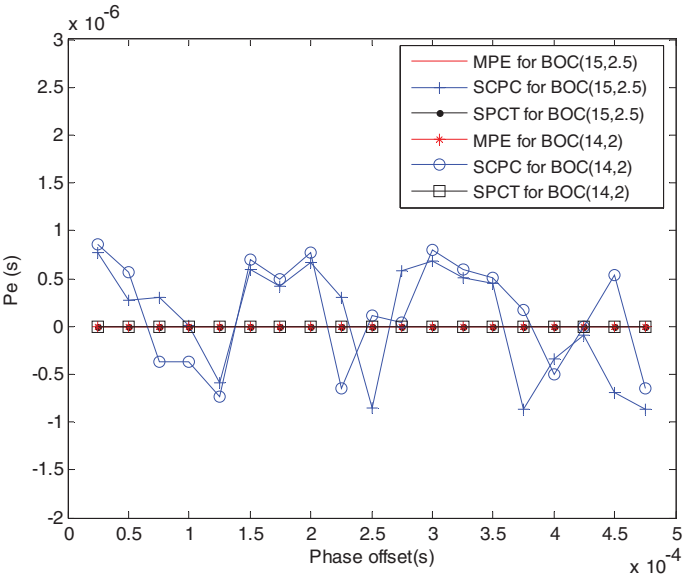

Figure 18. P_e results with changing phases of indirect signal.

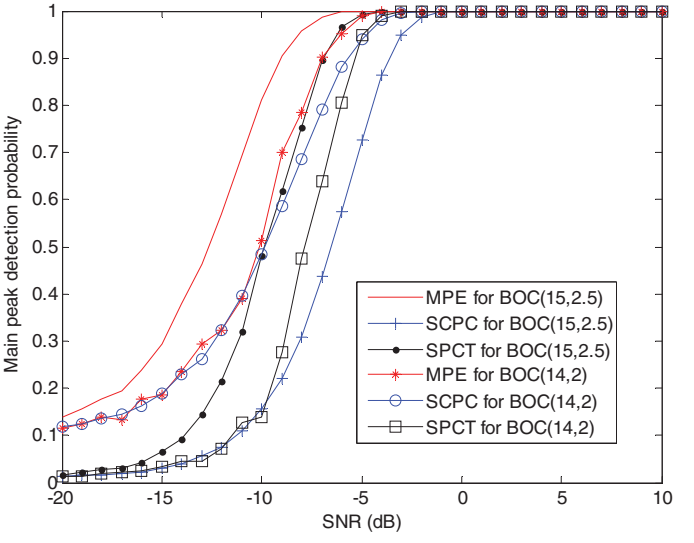

Figure 19. The main peak detection probability.

3.3. *Detection probability analysis.* Finally, the detection probability of the main and average side peaks is analysed under the condition of constant false alarm probability, which is 1×10^{-5}. The main peak detection probability results with changing SNR are shown in Figure 19. The results show that the main peak detection probability of the MPE method is better than that of the SCPC and SPCT methods. The side peak detection probability results with changing SNR are shown in Figure 20. The results show that the side

https://doi.org/10.1017/S0373463317000261 Published online by Cambridge University Press

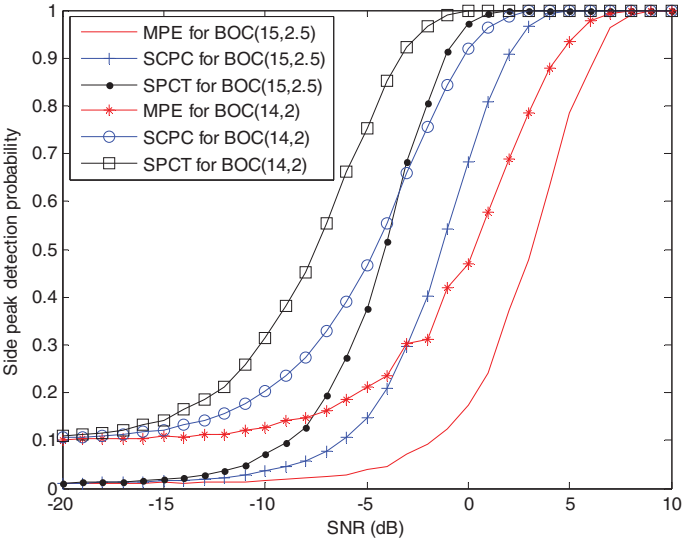

Figure 20. The side peak detection probability.

peak detection probability of the MPE method is lower than that of the SCPC and SPCT methods under the same condition. Thus, the MPE method's side peak cancellation ability is demonstrably the best.

4. CONCLUSIONS. In this paper, the problems involved with the large main peak estimation error and low correlation decision efficiency for high-order BOC signals are investigated, and the principles of several preferable estimation methods are studied, including the SCPC and SPCT methods. To solve the abovementioned problems, the MPE method is proposed. In this method, the synthesis cross-correlation function is established, and the geometry graph is formatted to calculate the main peak position and value. The side peaks can be cancelled in the MPE method, and the main peak can be extracted in the correct position. Furthermore, in the case of the MPE method, the detection probability of the main peak is the highest, the side peak detection probability is the lowest, and the phase estimation performance are noticeably better than those in the case of the SCPC and SPCT methods under the same test condition. Besides, the peak to average ratio of MPE method is the best under the same test condition, and it is twice that of SCPC and SPCT methods under the best test condition. The side peak cancellation ability of the MPE method is the best under the same test condition, and it is four to five times that of SCPC and SPCT methods under the best test condition.

ACKNOWLEDGMENTS

This work was supported by the National Natural Science Foundation of China (no. 61501309), the China Postdoctoral Science Foundation (no. 2015M580231), the Program for Liaoning Innovative Research Team in University (no. LT2011005).

REFERENCES

Burian, A., Lohan, E.S. and Renfors, M. (2006). BPSK-like methods for hybrid-search acquisition of Galileo signals. *in Proceedings of the IEEE International Conference on Communications*, Barcelona, Spain.

Brahim, F., Chonavel, T., Trubuil, J. and Boudraa, A.-O. (2015). Precise acquisition of global navigation satellite system signals in the presence of multipath and influence on tracking capability. *IET Radar, Sonar & Navigation*, **9**, 790–801.

Betz, J.W. (2001). Binary offset carrier modulations for radio navigation. *Navigation, the Journal of the Institute of Navigation*, **48**, 227–246.

Feng, S., Xu, G.H. and Xu, D.J. (2014). Unambiguous Acquisition Technique for Cosine-Phased Binary Offset Carrier Signal. *IEEE Communications Letters*, **18**, 1751–1754.

Feng, S., Xu, G.H. and Li, Q. (2015). Non-Coherent Unambiguous Tracking Method for Cosine-BOC Signals Based on an S-Curve Shaping Technique. *IEEE Signal Processing Letters*, **22**, 752–756.

Fine, P. and Wilson, W. (1999). Tracking algorithm for GPS offset carrier signals. *U.S Institute of Navigation, National Technical Meeting*, San Diego, CA.

Hodgart, M.S. and Simons, E. (2012). Improvements and Additions to the Double Estimation Technique. *2012 6th ESA Workshop on Satellite Navigation Technologies and European Workshop on GNSS Signals and Signal Processing*. Noordwijk, NL.

Heiries, V., Avila-Rodriguez, J., Irsigler, A.M., Hein, G., Rebeyrol, E. and Roviras, D. (2005). Acquisition performance analysis of composite signals for the L1 OS optimized signal. *In Proceedings of the ION GNSS International Technical Meeting of the Satellite Division*, Nashvile, Tennessee, US.

Julien, O., MacAbiau, C., Cannon, E. and Lachapelle, G. (2007). ASPeCT: unambiguous sine-BOC(n,n) acquisition/tracking technique for navigation applications. *IEEE Transactions on Aerospace and Electronic Systems*, **43**, 150–162.

Liu, H., Fang, S.J. and Wang, Z.B. (2015). Novel dual-band antenna for multi-mode GNSS applications. *Journal of Systems Engineering and Electronics*, **26**, 19–25.

Liu, Z., Pang, J., Liu, Y.X. and Wang, F.X. (2015). Double Strobe Technique for Unambiguous Tracking of TMBOC Modulated Signal in GPS. *IEEE Signal Processing Letters*, **22**, 2204–2208.

Mao, W.L., Hwang, C.S., Hung, C.W., Sheen, J. and Chen, P. H. (2013). Unambiguous BPSK-like CSC method for Galileo acquisition.*in Proceedings of the 18th International Conference on Methods and Models in Automation and Robotics*, Miêzyzdroje, Poland.

Martin, N., Leblond, V., Guillotel, G. and Heiries, V. (2003). BOC (x, y) signal acquisition techniques and performances. *U.S Institute of Navigation GPS/GNSS*, 188–198.

Sun, C., Zheng, H.L., Zhang, L.F. and Liu, Y. (2014). A Compact Frequency-Reconfigurable Patch Antenna for Beidou (COMPASS) Navigation System. *IEEE Antennas and Wireless Propagation Letters*,**13**, 967–970.

Sanghun, K., Dahae, C. and Seokho, Y. (2009). A new GNSS synchronization scheme. *In Proceedings of 2009 IEEE Vehicular Technology Conference –Spring*, Nanjing, China.

Ward, P.W. (2003). A design technique to remove the correlation ambiguity in binary offset carrier (BOC) spread spectrum signals.*59th Annual Meeting of the Institute of Navigation CIGTF 22nd Guidance and Test Symposium*, Albuquerque, NM, USA.

Yao, Z.L. and Feng, M. (2010). Unambiguous sine-phased binary offset carrier modulated *signal acquisition technique. IEEE Trans. Wireless Community,9, 577–580.*

Yao, Z., Cui, X.W., Lu, M.Q., Feng, Z.M. and Yang, J. (2010). Pseudo correlation-function-based unambiguous tracking technique for sine-BOC signals. *IEEE Transactions on Aerospace and Electronic Systems,* **46**,1782–1796.